THE ASTROPHYSICAL JOURNAL, 262:717–726, 1982 November 15

EXTREME ULTRAVIOLET SPECTROPHOTOMETRY OF THE HOT DA WHITE DWARF HZ 43: DETECTION OF He II IN THE STELLAR ATMOSPHERE

ROGER F. MALINA, STUART BOWYER, AND GIBOR BASRI
Space Science Laboratory and Astronomy Department, University of California, Berkeley
Received 1982 March 12; accepted 1982 May 18

ABSTRACT

We report a spectrum of the hot white dwarf HZ 43 in the extreme ultraviolet band from 170–500 Å with a resolution of 15 Å. The spectrum is marked by a prominent absorption edge at 225 Å ± 15 Å with N_λ (220 Å)/N(236 Å) = 0.51 ± 0.13. The observed edge is attributed to absorption at the 228 Å Lyman edge of singly ionized helium. A grid of blanketed LTE model atmospheres with uniform compositions of hydrogen with trace helium were used to interpret the data. We find that we are able to obtain satisfactory fits to our data for effective temperatures in the range 45,000–60,000 K either for pure hydrogen models with an interstellar He II column density in the range $(2.8–6)\times10^{17}$ ions cm^{-2}, or for models with a photospheric helium fractional number densities in the range $(1.5–6)\times10^{-5}$ of hydrogen. Our results, combined with observations at other wavelengths, yield a best estimate of 55,000–60,000 K for the effective temperature. We derive an upper limit on the interstellar column densities of $N(\mathrm{H}) \leq 2\times10^{17}$ cm^{-2} for neutral hydrogen, of $N(\mathrm{He\ I}) \leq 10^{17}$ cm^{-2} for neutral helium and of $N(\mathrm{He\ II}) \leq 6\times10^{17}$ cm^{-2} for singly ionized helium. However, no single pure hydrogen or uniform trace helium model will simultaneously fit the available optical to soft X-ray data. We have evaluated possible sources of He II in the interstellar medium and conclude that they are unlikely to contribute the entire observed column density. Hence the observations provide the first detection of helium in HZ 43.

Subject headings: interstellar: abundances — stars: abundances — stars: individual — stars: white dwarfs — ultraviolet: spectra

I. INTRODUCTION

The hot white dwarf Humason-Zwicky 43 ($\alpha_{1950} = 13^h14^m$, $\delta_{1950} = +29°22'$; $l^{II} = 54.2°$, $b^{II} = 84.2°$) has attracted renewed interest particularly since its discovery as the first star, other than the Sun, visible in the extreme ultraviolet band (Lampton *et al.* 1976). It has been extensively studied at optical (cf. Margon *et al.* 1976), far-ultraviolet (cf. Greenstein and Oke 1979), and soft X-ray wavelengths (cf. Bleeker *et al.* 1978). Recently it was observed spectroscopically from 500–800 Å using the *Voyager* UV spectrometer (Holberg *et al.* 1980). HZ 43 is in a wide binary system with a dM3.5e companion; the distance to the system is 65 ± 15 pc (Margon *et al.* 1976). The white dwarf is classified DA due to the presence of broad hydrogen lines and absence of helium lines in both the optical (Shipman 1972) and far-ultraviolet (Greenstein and Oke 1979). The most sensitive constraints on photospheric helium, the broad-band EUV fluxes and the absence of He II 4686 Å, yield a helium fractional number density limit of 10^{-3} to 10^{-6} of hydrogen (Auer and Shipman 1977). Determinations of the temperature have varied widely as a function of the wavelength of observation, method of analysis, and details of the model atmosphere used. Recent determinations in the optical and ultraviolet are bracketed by the range of 55,000–70,000 K determined by Auer and Shipman (1977). For instance, Wesselius and Koester (1978), applying the Kiel models to UV data, obtain $T_{\mathrm{eff}} = 61{,}000 \pm 5000$ K. Current atmospheric models, however, fail to reproduce the combined optical EUV and soft X-ray data (Heise and Huizenga 1980). Heise and Huizenga suggest that introducing a helium abundance varying with height in the photosphere resolves this discrepancy.

In this paper we report the first EUV spectrum of HZ 43 from 170–500 Å with a measurement of the He II 228 Å jump. If, as we argue, the detected helium is in the stellar photosphere, this provides the first direct measurement of the surface helium abundance of a DA white dwarf. Since EUV observations provide the most sensitive measurement of helium abundance in hot white dwarfs, it is possible that all DA white dwarfs have helium photospheric abundances at the level detected in HZ 43.

II. INSTRUMENTATION

The observations were carried out with a rocket-borne EUV imaging spectrometer (Malina 1979; Lampton *et al.* 1977) fed by a 38 cm diameter grazing-incidence tele-

scope. The telescope (Malina *et al.* 1980), an f/10 Wolter-Schwarzchild type II system, was figured by diamond-turning a copperplated aluminum blank. The mirror surfaces consisted of evaporated gold over a polished nickel substrate. The on-axis image was ~6″ FWHM in visible light and better than 15″ in the EUV as determined in flight. The intrinsic aberrations of the design dominated the fabrication errors beyond 1.5 off axis, reaching 1′ rms radius at 5′ off axis.

The telescope fed a grazing-incidence spectrometer housed in an evacuated box. The vacuum box entrance was sealed with a movable 1500 Å thick aluminum filter whose transmission exceeded 10% from 170 Å to 600 Å. When in place, the filter eliminated potential contamination from geocoronal Lyman-alpha radiation and residual gas within the sounding rocket shell. The spectrometer design was based on a novel type III concave holographic grating (Flamand, Passereau, and Thevenon 1977) mounted in the converging beam from the optics. The grating was ruled at 1834 l mm^{-1} yielding a plate factor of 6.4 Å mm^{-1}. The detector was a ranicon (Lampton and Paresce 1974) consisting of a cascaded pair of microchannel plates whose output pulse was proximity focused to a two-dimensional resistive anode readout system. The front channel plate was coated with magnesium fluoride and was cut at a bias angle of 40° in order to obtain high quantum efficiency in this grazing-incidence application. The instrument electronics digitized the position of the detector counts in a 256 by 256 channel image which was telemetered to ground and recorded.

The instrument was calibrated relative to a channel electron multiplier transfer recording standard (Mack, Paresce, and Bowyer 1976) that has been calibrated against a National Bureau of Standards windowless diode. The results of the on-axis calibration of the

TABLE 1

HZ 43 FLUXES (filtered data)

λ (Å)	Background Counts	Signal Counts	Source[a] Counts	Δλ[b] (Å)	A_{eff} (cm^2)	$F\nu$[c] (obs)	Atmospheric Transmission	$F\nu$[c] (corr)	Error[c,d]
176 ...	43	66	−26	18	0.60	...	...	[e]	...
192 ...	36	48	12	16	0.65	...	...	[e]	...
208 ...	53	103	50	14	0.68	6.8	0.91	7.5	1.8
220 ...	38	90	52	14	0.68	7.5	0.90	8.3	1.7
236 ...	39	141	101	14	0.67	16	0.89	18	3
250 ...	35	135	99	14	0.64	17	0.87	20	3
268 ...	23	119	95	13	0.62	20	0.86	23	3
289 ...	24	128	103	12	0.59	25	0.85	30	4
292 ...	22	95	72	11	0.58	21	0.84	25	4
302 ...	16	100	83	10	0.55	27	0.83	32	3
312 ...	29	105	75						
320 ...	11	92	81	9	0.52	33	0.82	40	4
330 ...	17	92	74						
338 ...	20	64	43	9	0.5	24	0.80	29	4
348 ...	17	73	55						
357 ...	15	73	57	9	0.47	31	0.79	38	4
365 ...	11	68	56						
373 ...	9	66	56	9	0.44	36	0.78	46	6
385 ...	19	86	66						
345 ...	16	76	59	9	0.41	32	0.77	41	5
401 ...	14	52	37						
409 ...	17	61	43	9	0.39	29	0.77	37	6
417 ...	15	48	42						
422 ...	14	66	50	9	0.37	33	0.76	43	7
430 ...	17	42	23						
443 ...	13	50	35	10	0.33	26	0.76	35	7
456 ...	17	45	25						
467 ...	15	76	52	11	0.29	37	0.75	49	8
480 ...	20	62	32						
490 ...	29	83	44	12	0.26	39	0.75	52	12
504 ...	51	95	34						

[a]Signal minus background, corrected for second order.

[b]Bin size. Resolution is 15 Å

[c]Units are in mfu = 10^{-26} ergs cm^{-2} s^{-1} Å^{-1}.

[d]Error (1 σ) from counting statistics in mfu. Systematic error is estimated at ±20% including calibration and atmospheric transmission uncertainties.

[e]Absolute flux unreliable due to edge effects of detector and cutoff of filter.

effective area, $A_{\rm eff}$, are given in Table 1. Systematic uncertainties, which dominate measurement errors, are estimated at ±20%. The calibration was repeated end-to-end before and after flight; no changes were found at the 20% level. The wavelength resolution of the spectrometer is a convolution of the aberrations of the spectrometer, the image blur due to the optics and the detector resolution. In flight the spectral image is further broadened by the pointing system jitter and off-axis aberrations resulting from pointing offsets. The wavelength resolution in flight was determined empirically by measuring the stellar image profile and was found to correspond to 15 Å FWHM.

III. OBSERVATIONS

The instrument was launched at 0900 hrs MST on 1978 April 10 from the White Sands Missile Range. The observing program consisted of two inertial guidance system updates on Arcturus and Capella, followed by two 105 s observations of HZ 43. The first observations of HZ 43 was carried out from an altitude of 200 km and continued until apogee at 300 km; during this observation the aluminum filter was in the spectrometer aperture. The source was detected at a count rate of 21 to 24 counts s^{-1} above a total detector background rate of 30 counts s^{-1}. During the observation, the count rate rose by 15% reflecting the decreasing atmospheric attenuation for the source zenith angle of 45°. Following the removal of the aluminum filter, HZ 43 was re-observed during the descent. The source was then detected at a count rate of 46 counts s^{-1} above a total detector background rate of 650 counts s^{-1}. The enhanced background is attributed to geocoronal Lyman-alpha radiation scattered within the instrument; this radiation was successfully attenuated by the aluminum filter during the first observation.

In Table 1 we summarize the filtered HZ 43 data. The unfiltered data has been analyzed elsewhere (Malina 1979) and was found to be consistent, given the poorer statistics, with the filtered data. In Table 1 the detector channels have been binned and summed into histograms for the source and background spectra. The background spectrum, with an average count rate of 4.5 counts s^{-1}, was obtained simultaneously from a strip of the detector not exposed by the source spectrum. This background strip was found to have the same count rate and spectral distribution as the spectrum strip when a source was not being observed. In Figure 1 we show the HZ 43 spectrum after subtraction of the background and grouping into wavelength resolution elements. The spectrum shown in Figure 1 has not been corrected for second or higher order images which contribute counts longward of 340 Å.

We find that HZ 43 was detected at greater than 2 σ in every resolution element from 200 Å to 500 Å. No significant emission or absorption lines are found with a 3σ upper limit of 10 Å equivalent width. The spectrum exhibits a significant decrease in flux shortward of 225 ± 15 Å; this decrease in flux occurs within two resolution elements or 30 Å. The reality of this jump is supported by its presence in second order at ~460 Å. The size of the absorption jump is $N(220\ \text{Å})/N(236\ \text{Å}) = 0.51 \pm 0.13$, where the indicated 1 σ error is derived from Poisson statistics. A similar analysis of the unfiltered data yields $N(220\ \text{Å})/N(236\ \text{Å}) = 0.7 \pm 0.4$ (Malina 1979).

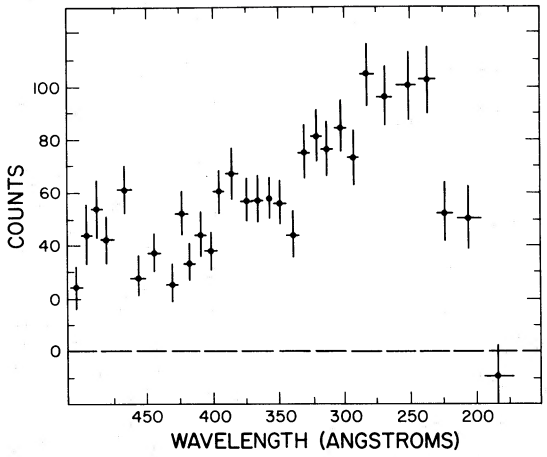

FIG. 1.—Count spectrum of HZ 43 obtained with the aluminum filter in place. The detector bins have been grouped into wavelength resolution elements, corrected for background, and rectified using the wavelength calibration. One sigma statistical error bars are shown. The absorption edge attributed to He II is seen at ~225 Å and in second order at ~460 Å.

In Table 1 and Figure 2 we present the reduced spectrophotometry after conversion to absolute fluxes and correction for atmospheric attenuation. The higher order images have been subtracted using the calibrated higher order grating efficiencies (Malina 1979). The atmospheric transmission summarized in Table 1 has been calculated using the models of Jacchia (1971) as specified by the solar and geomagnetic activity indices at the time of launch. The dominant source of attenuation is continuous opacity of N_2 and O_2; hence, no spectral features are contributed to the observed spectrum. Also shown in Figure 2 are a selection of UV and optical fluxes, as well as the *Apollo-Soyuz* broad-band EUV fluxes (Lampton *et al.* 1976) and the *Voyager* spectrum (Holberg *et al.* 1980). Our fluxes are in good agreement with the aluminum filter band flux given by Lampton *et al.* (1976) but indicate a steeper spectrum than expected from their beryllium filter band. Although our bandpass and that of the *Voyager* spectrometer do not overlap, extrapolations of each data set to 500 Å are consistent with each other within the stated uncertainties. The soft X-ray measurements of Bleeker *et al.* (1978) are not shown since the absolute fluxes determined from

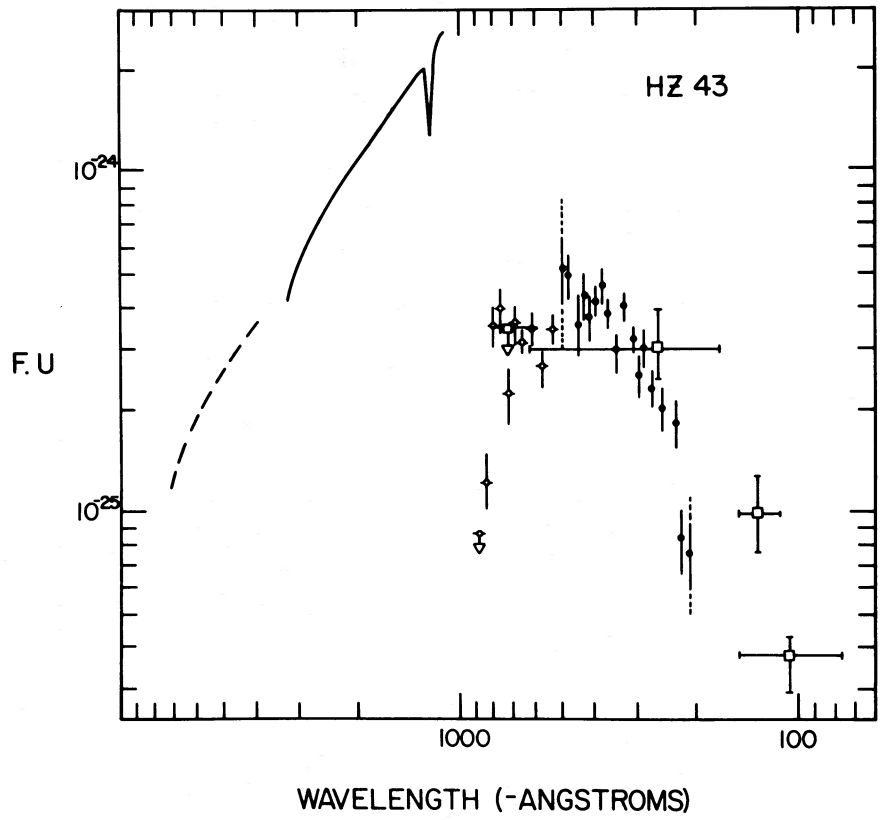

FIG. 2.—Combined optical, UV, and EUV spectrum of HZ 43. Data are: *dashed line*, Margon *et al.* 1976; *solid line*, Greenstein and Oke 1979; *open circles*, Holberg *et al.* 1981; *squares*, Lampton *et al.* 1976; *solid circles*, this paper. The data from this observation are shown with $\pm 1\ \sigma$ statistical error bars (*solid line*) and the typical $\pm 20\%$ estimated systematic uncertainty (*dotted extension to error bars*).

their proportional counter measurements are model dependent.

IV. ANALYSIS

a) Origin of the 225 Å Feature

We identify the decrease in flux shortward of 225 Å with absorption at the 228 Å Lyman limit of single ionized helium. The observed jump implies an absorption column density of $(2.8\text{–}6.0)\times 10^{17}$ He II ions cm^{-2}, assuming a cross section of 1.6×10^{-18} cm^2 (Lang 1974). *A priori*, this He II could be located in the white dwarf photosphere, the interstellar medium, or in the solar system.

Sources of He II within the solar system include the Earth's plasmasphere, the solar wind, and the interplanetary medium. The column density in the plasmasphere can be derived from observations of backscattered ~ 304 Å radiation in the illuminated portion of the plasmasphere and yields maximum column densities of 10^{12}–10^{13} ions cm^{-2} (Chiu *et al.* 1979). Within the Earth's shadow cone, upper limits on the 304 Å flux imply a maximum column density of 10^9 ions cm^{-2} due to the solar wind (Paresce, Fahr, and Lay 1981). Thus the observed He II must be beyond the solar system.

A direct proof of a photospheric origin for the jump could be obtained by observing pressure broadening in either the absorption edge or the helium resonance lines. This has been done for hydrogen in HZ 43 in which the hydrogen Lyman-alpha line has been found to be broadened to a half-width of 35 Å (Greenstein and Oke 1979). The corresponding lines in He II, which is hydrogenic, will be narrower in wavelength by a factor of $\sim Z^5$ (Mihalas 1978; Griem 1974). The numerical estimate of the last resolvable line in the series using the Inglis-Teller formula (Griem 1974) confirms that pressure broadening is not detectable with the available resolution of 15 Å. Since the origin of the He II cannot be determined on these grounds, we have used model stellar atmospheres attenuated by an intervening interstellar medium to fit to the data.

b) Models

We have computed atmospheres for HZ 43 using a linearization code provided to us by L. Auer (cf. Auer and Shipman 1977) and modified to include hydrogen

line blanketing. The model is LTE; this assumption has been shown to be a good approximation in this temperature regime (Wesemael *et al.* 1980). The composition employed was hydrogen with uniform trace helium; as we show below, these models are adequate to describe the observed spectral shape. We required that the temperature corrections converge to 0.1%, with a corresponding radiative flux convergence of 1%. We have used models with hydrogen line blanketing because, apart from being physically more realistic, they provided significantly better fits to the data for $T_{\rm eff} \leq 60{,}000$ K. Effects of helium line blanketing have not been included as they are expected to be small since helium is present only in trace amounts; in addition, the helium lines are narrow and are strongest far from the peak of the Planck spectrum. Log $g = 8$ has been used in all cases since the continuum fluxes are insensitive to this assumption (Auer and Shipman 1977), and it is consistent with estimates of the HZ 43 surface gravity (Shipman 1979). Our code is similar to that described by Wesemael *et al.* (1980); we have checked several models against his results for pure hydrogen and against models in Wesemael (1981) which contain some helium. The results always agreed to within 5%, although we found that the EUV fluxes were very sensitive to the details of the depth and frequency grids employed because both the opacity and source function are very sensitive to temperature changes in this frequency range (cf. Böhm and Kapranidis 1980). These fluxes must therefore be regarded as somewhat less certain and are subject to the greatest disagreement with other codes, than at other wavelengths.

The results of our model atmosphere calculations are illustrated in Figure 3 where we have plotted the size of the helium jump H_λ (228$^+$ Å/228$^-$ Å) as a function of effective temperature for trace helium abundances of 10^{-5}, 5×10^{-5}, and 10^{-4} of hydrogen. Although our continuum fluxes agreed with those of Wesemael (using the same method), we found substantially greater discrepancies with the He II continuum jumps given by Heise and Huizenga (1980). Our calculated He II jumps were consistently larger, with the discrepancy increasing from 10% at helium densities of 10^{-5} to 50% at helium densities of 10^{-4}. It is difficult to determine the origin of this difference, but we suspect that different approximations must be used in the model atmosphere treatment.

We have convolved the atmospheric model described above with attenuation by a two-component interstellar medium. The two components are a neutral ISM of mean density n_1, with cosmic abundances and cross sections σ_1 from Cruddace *et al.* (1974), and an independent ISM column of He II density n_2 and cross section σ_2. The hydrogen associated with the He II is assumed to be fully ionized and hence does not contribute to σ_2. The opacity due to the metals associated with the He II is ignored.

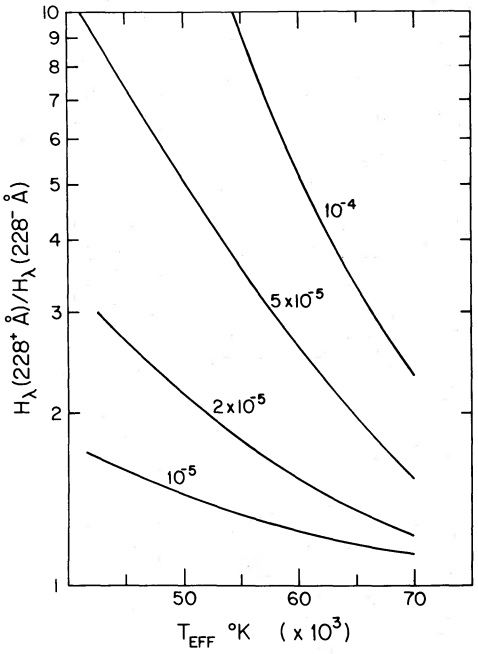

FIG. 3.—The size of the He II 22 Å jump as a function of photospheric temperature and fractional helium abundance by number. Lines of constant helium number density, $N(\mathrm{He})/n(\mathrm{H})$, are labeled.

The predicted flux in photons cm^{-2} s^{-1} Å^{-1} at Earth at a given wavelength, λ, is then determined from the relation

$$f\lambda = \frac{4\pi R_\odot^2}{d^2}\left(\frac{R_*}{R_\odot}\right)^2 \dot{H}_\lambda(T_{\rm eff}, n_{\rm He}/n_{\rm H}) \times \exp-(n_1\sigma_1 d + n_2\sigma_2 d), \quad (1)$$

where R_* is the stellar radius, d is the distance to HZ 43, and H_λ is the emergent Eddington flux from the stellar surface as a function of the effective temperature, $T_{\rm eff}$, and the fractional helium abundance, $n_{\rm He}/n_{\rm H}$. Models were computed for a range of temperatures from 45,000 K to 70,000 K.

c) *Photospheric Helium Models*

We first consider the scenario where the observed He II all originates in the stellar photosphere by setting $n_2 = 0$. Increasing helium density first results in the appearance of the 228 Å jump for $n_{\rm He}/n_{\rm H} \geq 5\times10^{-6}$ as can be seen in Figure 3. The redistribution of flux shortward of 228 Å then leads to significant changes in both the slope and absolute intensity of the EUV spectrum, while leaving the UV and optical flux distributions almost unaffected. We test the calculated model against our 170–500 Å EUV data using the χ^2 statistic (see Lampton, Margon, and Bowyer 1976) and obtain

TABLE 2

HZ 43 PARAMETER DETERMINATIONS

PARAMETER	THIS EXPERIMENT[a] Case 1	THIS EXPERIMENT[a] Case 2	HOLBERG *et al.*	AUER AND SHIPMAN	HEISE AND HUIZENGA	WESSELIUS AND KOESTER
$T_{\rm eff}$ (K)	$(45–60)\times10^3$	$(45–64)\times10^3$	55×10^3	$(55–70)\times10^3$	60×10^3	$(55–65)\times10^3$
$R/R_\odot$	0.018–0.0065	0.018–0.0062	0.0146	0.0146–0.0133	0.0113–0.0086	0.018–0.009
He/H	$(1.5–6)\times10^{-5}$	$\leq6\times10^{-5}$	H only	10^{-6}–10^{-3}	Layered	10^{-5}–10^{-3}
N_1(H) ($\rm cm^{-2}$)	$\leq2\times10^{17}$	$\leq1.7\times10^{17}$	$(1.9–5.8)\times10^{17}$	$(0.63–2.4)\times10^{18}$	$\leq2\times10^{18}$	...
n_1 ($\rm cm^{-3}$)	≤0.001	≤0.0009	0.001–0.003	0.0034–0.013	≤0.01	...
N_2(He II) ($\rm cm^{-2}$)	...	$\leq6\times10^{17}$	...	...	...	...

[a]All parameter ranges for this experiment are quoted for 90% confidence joint estimation.

the χ^2 contours for joint estimation of the four free parameters $T_{\rm eff}$, $n_{\rm He}/n_{\rm H}$, R_*, and n_1. The assumed errors in the data are the $N^{1/2}$ counting errors listed in Table 1 and exclude estimated systematic uncertainties.

The results are summarized as Case 1 in Table 2 and are also displayed in the left panel of Figure 4 as a map of χ^2 in the two-dimensional space $T_{\rm eff}$, $n_{\rm He}/n_{\rm H}$. We obtain acceptable fits for all models within the areas indicated in Figure 4 by 90% and 99% confidence contours. Our determination of the temperature overlaps those of other observers and leads to a best estimate of $55{,}000\ {\rm K} \leq T_{\rm eff} \leq 60{,}000$ K. For this temperature range we derive that the photospheric helium number density lies in the narrow range $(2.5–6)\times10^{-5}$ of hydrogen. We set an upper limit on the neutral ISM component of 2×10^{17} $\rm cm^{-2}$, consistent with, but lower than, the upper limit set by Holberg *et al.* (1980). Our determination of the stellar radius from our 170–500 Å data, overlaps that of other observers as shown in Table 2. However, the required radius is systematically smaller by 30%–50% at a given model effective temperature than that determined from optical and UV data. This discrepancy is larger than can be accounted for by the estimated uncertainty in our absolute calibration and is most severe shortward of 300 Å.

d) *Models With Interstellar* He II

We consider next models that include interstellar helium as a contributor to the observed He II edge. The model is identical to Case 1 except that n_2, the ISM He II number density, is allowed to vary freely. The results are summarized as Case 2 in Table 2. We give the derived constraints on the interstellar He II column in the right panel of Figure 4 as a map of χ^2 in the two-dimensional space $T_{\rm eff}$, $N_{\rm He}/n_{\rm H}$. We obtain acceptable fits within indicated contours for 90% and 99% confidence levels for joint estimation of the five parameters. Also shown in Figure 4 are contours of required interstellar He II column density. As for Case 1 we find

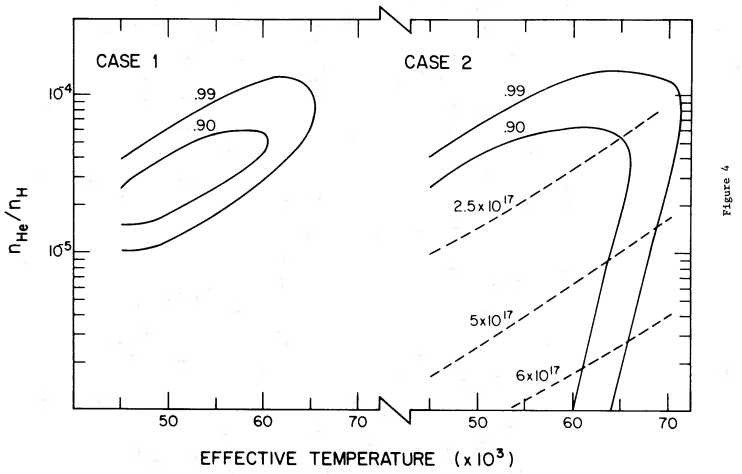

Figure 4

FIG. 4.—Results of model fitting to the EUV spectrum. Contours of constant χ^2 for 90% and 99% confidence for joint estimation of the parameters are shown as a function of surface helium abundance and effective temperature: (*left panel*) Case 1 photospheric He II only. Case 2 (*right panel*): photospheric and interstellar He II allowed. Contours of constant interstellar He II column are shown as a dashed line and are labeled in $\rm cm^{-2}$.

that the required stellar radii are 30%–50% smaller at a given temperature than deduced from optical or UV data. As can be seen in Figure 4, models with an interstellar He II column density ranging from 0 to 6×10^{17} ions cm^{-2} fit the data as long as the stellar photosphere contributes the balance of the observed 228 Å jump. In particular, pure hydrogen models with $T_{\rm eff} \leq$ 65,000 K provide an acceptable fit provided an ISM He II column density of $(2.8–6)\times10^{17}$ ions cm^{-2} is present. We find that the additional parameter n_2 results in a reduction of ~1 in the χ^2, an improvement significant only at the 68% level. Thus we cannot conclude that an interstellar component of He II is required. We can, however, set a firm upper limit on the interstellar He II column density of 6×10^{17} ions cm^{-2}.

V. DISCUSSION

a) *Photospheric Models*

We have found that models with trace helium will provide acceptable fits to our data. Pure hydrogen models will also provide acceptable fits provided the observed He II column density is located in the ISM. This conclusion is consistent with those of observers at longer wavelengths who obtain satisfactory fits with pure hydrogen models. However, no single model will simultaneously fit all the data longward of 200 Å because of the discrepancy in absolute scaling factors. For a $T_{\rm eff} =$ 60,000 K pure hydrogen model we find $0.0075 \leq R/R_\odot \leq 0.008$ compared to the $0.010 \leq R/R_\odot \leq 0.016$ quoted by Shipman (1979) also for $T_{\rm eff} = 60{,}000$ K. We also find that, in addition to this 50% discrepancy in absolute fluxes, the largest difference occurs primarily in the 300–228 Å band implying a wavelength dependent discordance. A similar problem occurs for the soft X-ray band where Heise and Huigenza (1980) were unable to obtain satisfactory fits using either pure hydrogen or uniform trace helium models. Although those authors did not consider attenuation due to interstellar He II, their conclusion is likely to be unaffected since the effects of the required He II column density are small shortward of 100 Å. However, we have found that the EUV and soft X-ray fluxes are extremely sensitive to the computational details employed so that caution should be used in comparing results from analysis with differing models.

The low metal abundance in DA white dwarfs is believed to be caused by gravitational settling in the presence of the strong gravitational field (Schatzman 1958). The success of competing mechanisms, such as accretion, convective mixing, and radiation pressure will determine the relative abundances of the trace elements relative to hydrogen. A few white dwarfs are now known to have both hydrogen and helium in their atmospheres (Liebert *et al.* 1979) with the hottest ones covering the largest range in helium to hydrogen ratio. Our determination of $n_{\rm He}/n_{\rm H} = (2.5–6)\times10^{-5}$ for $T_{\rm eff} =$ 55,000–60,000 K, assuming no interstellar He II, provides the lowest measurements of the helium density in a white dwarf and provides a stringent test for theories of the formation of hybrid white dwarfs.

Heise and Huizenga (1980), in discussing the soft X-ray data of Bleeker *et al.* (1978), proposed a layered atmosphere consisting of a pure hydrogen layer on top of a helium-rich atmosphere. Such a scenario may be physically plausible depending on the time scales and effectiveness of the various mechanisms competing with gravitational diffusion. The particular model proposed by Heise and Huizenga (1980) does not fit our data because it predicts an insufficient 228 Å jump. However, as these authors noted, the soft X-ray data do not uniquely define a layered model since all models with $n_{\rm He}/n_{\rm H} \gtrsim 0.05$ below $5 \leq \tau_{\rm H} \leq 15$ gave acceptable fits. Muchmore (1982) has discussed in detail the numerical difficulties encountered in modeling layered models; he concludes that a predicted discontinuous temperature inversion does physically occur leading to a much smaller 228 Å jump at a given effective temperature. However, he points out that it is only possible to distinguish layered atmospheres from uniform ones on the basis of the continuum spectra both longward and shortward of 228 Å. The combined data now available motivates further theoretical models which realistically describe element gradients in the stellar photosphere.

b) *The Local Interstellar Medium*

Our observations of the line of sight to HZ 43 constrain the column density of neutral hydrogen to N_1(H) $\leq 2\times10^{17}$ cm^{-2} and singly ionized helium to N_2 (He II) $\leq 6\times10^{17}$ cm^{-2}. In addition our data shortward of 504 Å, together with the *Voyager* observations longward of 504 Å, imply $F_\lambda(504^-\ \text{Å})/F_\lambda(504^+\ \text{Å}) \geq 0.5$ or N(He I) $\lesssim 10^{17}$ cm^{-2}, assuming a 50% uncertainty in the relative absolute calibrations of the two experiments. These limits impose useful constraints on conditions in the local interstellar medium.

The local interstellar medium is known to be a very patchy (cf. Cash, Bowyer, and Lampton 1978; Knude 1979) with evidence for the existence of several small clouds with n(H I) ~ 10 cm^{-3} embedded within a warm intercloud medium (Crutcher 1982); additional evidence indicates the presence of one or more H II regions with $T \geq 2\times10^5$ K (e.g., York and Kinahan 1979). Components of hot gas are also seen in the soft X-ray and EUV backgrounds (Paresce and Stern 1981). Our limits on neutral gas rule out the presence of any clouds with n (H I) $= 10$ cm^{-3} larger than ~ 0.01 pc along the line of sight to HZ 43. This result is consistent with the absence of nearby clouds in the direction of the north galactic pole as indicated from reddening (Knude 1979) and polarization measurements of nearby stars (Tinbergen 1982).

The local warm intercloud medium is known to impinge on the solar system since it has been observed as an interstellar wind in solar backscattered 1216 Å and 584 Å radiation. The gas is known to extend tens of parsecs in some directions through observations in UV (Frisch 1981) and optical absorption lines (Crutcher 1982). The gas is characterized by $T = 9000$–$15{,}000$ K, $n(\text{H I}) = (4\text{–}6) \times 10^{-2}$ cm^{-3} and $n(\text{He I}) = (1.1\text{–}2.7) \times 10^{-2}$ cm^{-3} (Weller and Meier 1981). Our limits on neutral hydrogen and helium imply that in the direction of HZ 43 the local warm intercloud medium extends 2–3 pc at most. Thus the bulk of the line of sight must be very low density, with $n(\text{H I}) < 0.001$ cm^{-3}. If this gas is in pressure equilibrium with the local interstellar wind, which has a pressure of $nT \approx (3.6\text{–}9) \times 10^2$ cm^{-3} K, it must be either hot or highly ionized by an external ionizing source. This implies that the neutral hydrogen column density of $\sim 2 \times 10^{20}$ cm^{-2} seen in 21 cm in the direction of HZ 43 (Heiles 1975) must be all located beyond the star. Alternatively, considerable patchiness exists in the local ISM, on a scale smaller than the radio beam, allowing a clear line of sight to HZ 43.

c) He II *in the Warm and Hot ISM*

We examine next possible sources of He II in the interstellar medium in order to determine on theoretical grounds whether an interstellar origin is plausible.

The helium in the interstellar wind, including effects of ionization due to local radiation field, is expected to be predominantly neutral; detailed calculations indicate that $n(\text{He II})/n(\text{He I}) \leq 10^{-3}$ for the measured temperature (cf. Blum and Fahr 1976; Weller and Meier 1981). Assuming the 3 pc upper limit derived above for the extent of the interstellar wind toward HZ 43 and the observed local He I density, the interstellar wind can contribute only 2.5×10^{14} He II ions cm^{-2}, or 10^{-3} of the observed He II column density.

For hot ISM gas, such as the O VI bearing phase with $T \geq 10^5$ K or the soft X-ray emitting gas with $T \geq 10^6$ K, the helium will be predominantly doubly ionized. The calculations of Shapiro and Moore (1976) indicate that in both steady state and time dependent cooling scenarios the fraction $n(\text{He II})/n(\text{He I} + \text{He II} + \text{He III})$ is less than 0.1% for temperatures above 10^5 K. A He II bearing hot gas with $n(\text{He II}) = (2.8\text{–}6) \times 10^{17}$ cm^{-2}, assuming a near unity filling factor, would have a pressure exceeding 2×10^4 cm^{-3} K and be far out of pressure equilibrium with the local interstellar wind. Assuming the steady state ionization conditions of Shapiro and Moore (1976), this gas would also contain associated column densities of C IV of at least 4×10^{15} cm^{-2} and of Si IV of at least 10^{14} cm^{-2}. These column densities exceed by an order of magnitude the column densities observed in nearby stars (cf. Cowie, Taylor, and York 1981). A less pervasive gas which might have avoided detection in front of other nearby stars is implausible because of the large implied overpressure. We conclude that if the He II observed in the spectrum of HZ 43 is interstellar in origin, it must arise in gas with intermediate gas temperatures or else in a gas with ionization conditions that enhance He II.

d) He II *in an Intermediate Temperature ISM*

Intermediate temperature gas has been detected in various locations including the galactic corona, interfaces between clouds and hot ISM, and in interstellar shocks. In the nearby ISM, York and Kinahan (1979) have found weak evidence for gas at $\sim 8 \times 10^4$ K along the line of sight to α Virginis which is presumably an intermediate temperature region distinct from the gas producing the O VI absorption. Bruhweiler and Kondo (1981) have identified gas with ionization levels characteristic of gas with $T = 5\text{–}12 \times 10^4$ K along the line of sight to the nearby hot dwarf G191-B2B. A possible scenario for the presence of intermediate temperature gas is that a nearby supernova in the Sco-Oph association has shocked local ISM (Weaver 1979) which is now cooling. In a time dependent cooling scenario, ions of a O VI, Si III, Si IV, C III, and C IV remain frozen at intermediate temperatures. Using the calculations of Shapiro and Moore (1976), the observed He II column density would imply $N(\text{H II}) \geq 10^{14}$ cm^{-2}, $N(\text{O VI}) \geq 10^{14}$ cm^{-2}, $N(\text{Si III}) \geq 3 \times 10^{13}$ cm^{-2}, and $N(\text{C IV}) \geq 5 \times 10^{14}$ cm^{-2}. These predicted column densities exceed those observed in nearby stars (Cowie *et al.* 1981) and are several times higher than those observed by Bruhweiler and Kondo (1981). Preliminary results (Malina, Basri, and Bowyer 1982) of a search for these ions in the spectrum of HZ 43 using *IUE* provide upper limits to the column densities at, or below, the detection levels of Bruhweiler and Kondo (1981).

A more localized source of steady state intermediate temperature gas would occur in the conductive interfaces between the coronal gas and interstellar clouds. Using the calculations of McKee and Cowie (1977), the He II column density on an individual cloud can be evaluated as $N(\text{He II}) \lesssim 2 \times 10^{14} T_{f6}^{-3/2} n_{-2} R_{\text{pc}}$ cm^{-2}, where T_{f6} is the asymptotic gas temperature in units of 10^6 K, n_{-2} is the asymptotic hot gas density (in units of 10^{-2} cm^{-3}), and R_{pc} is the maximum dimensions of the cloud. Assuming hot intercloud medium parameters of $T \sim 10^6$ K, $n \sim 10^{-2}$ cm^{-2}, and R ~ 10 pc, an implausible 20 interfaces would be needed to explain the observed column density. In addition, the line of sight would be required to cross the interface, avoiding the neutral cloud cores.

He II is expected to be formed in the intermediate velocity interstellar shocks observed in Si III. Cohn and York (1977) found that high velocity interstellar ions were present in about 30% of the stars they observed out to 2 kpc, thus one such shock could be postulated to lie

along the line of sight to HZ 43. Extensive calculations have been carried out by Shull and McKee (1979) that yield $N(\text{He II}) \approx 7.5 \times 10^{15}$ cm^{-2} for an 80 km s^{-1} shock, this rises to $N(\text{He II}) \approx 2.4 \times 10^{17}$ cm^{-2} for a 130 km s^{-1} shock (both cases assume the shock advances into an ambient medium of density 10 cm^{-3}). Our limits on the neutral hydrogen column indicate that a postulated shock would be advancing into ambient ionized material with $n \ll 10$ and the predicted shock $N(\text{He II}) \ll 10^{17}$ cm^{-2}.

We conclude that the column density of intermediate temperature gas, required to account for the observed He II are too large to be explained by any of the known sources in the nearby ISM.

e) *Circumstellar* He II

Bruhweiler and Kondo (1981) have reported detection of N V, C IV, and Si IV in the spectrum of the nearby hot white dwarf G191-B2B; they argue that the least problematical origin for these lines is in a halo associated with the white dwarf. However, as they point out, an origin of these ions in a planetary type nebula is implausible because neither the available photoionizing flux nor the expanding shock, as estimated above, can provide the necessary column densities. A coronal origin for the observed He II can be ruled out for HZ 43 since the helium jump is seen in absorption; any optically thin corona hotter than the photosphere would lead to a helium jump seen in emission (cf. Muchmore and Böhm 1978).

VI. CONCLUSIONS

We have presented the first spectrum of HZ 43 in the 200–500 Å band. The spectrum is marked by a prominent edge at 225 Å ± 15 Å which we attribute to absorption by intervening singly ionized helium. We have fitted model atmospheres with both pure hydrogen and hydrogen with trace helium to the data. For atmospheres with hydrogen and trace helium we find that models with acceptable fits have a helium photospheric fraction of $(1.5–6) \times 10^{-5}$ of hydrogen for a photospheric temperature in the range of 45,000–60,000 K. In the case of a pure hydrogen photosphere we require an interstellar He II column density of $(2.8–6) \times 10^{17}$ ions cm^{-2}. Although in both cases we are able to fit the models to the observed slope and spectral features, we find that a single uniform abundance model is unable to fit simultaneously the available optical, UV, and EUV data. This discrepancy appears to be larger than can be accounted for by the published uncertainties in absolute calibrations of the EUV data. The conclusion that uniform abundance models inadequately describe the spectrum of HZ 43 is supported by a similar conclusion for fits to the soft X-ray data (Heise and Huizenga 1980).

Our limits on the interstellar neutral hydrogen column density of 2×10^{17} cm^{-2} indicate that the local interstellar wind extends only a few parsecs towards HZ 43 and that the rest of the line of sight is characterized by $n(\text{H I}) \leq 0.001$ cm^{-3}. We have evaluated possible interstellar sources of He II and conclude that the entire observed He II is unlikely to be interstellar unless it is peculiar to the line of sight to HZ 43. Neither the hot nor the warm phases of the ISM will contribute significant column densities; intermediate temperature or high ionization components of the local ISM can also be ruled out given our current understanding of the local ISM. We cannot, however, rule out that significant He II interstellar column of a few 10^{16} ions cm^{-2} is present in the line of sight to HZ 43.

We thank F. Paresce, R. Kimble, M. Lampton, G. Penegor, and W. Cash for assistance in the development of the payload; J. Bryan of the Lawrence Livermore Laboratories for the fabrication of the EUV optics; J. Heise, L. Auer, H. Shipman, and F. Wesemael for material prior to publication; M. Schull and C. McKee for discussions; and Galileo Electro Optics for providing the microchannel plates. We also thank NASA-GSFC sounding rocket divisions and the White Sands Missile Range crew for the flawless launch of 27-026, The Blue Rainbow. This research has been supported by NASA grant NGR-05-003-450.

REFERENCES

Auer, L. H., and Shipman, H. L. 1977, *Ap. J.* (*Letters*), **211**, L105.
Bleeker, J. A. N., *et al.* 1978, *Astr. Ap.*, **69**, 145.
Blum, P. W., and Fahr, H. J. 1976, *Ap. Space Sci.*, **39**, 321.
Böhm, K. H., and Kapranidis, S. 1980, *Astr. Ap.*, **87**, 307.
Bruhweiler, F. C., and Kondo, Y. 1981, *Ap. J.* (*Letters*), **248**, L123.
Cash, W., Bowyer, S., and Lampton, M. 1979, *Astr. Ap.*, **80**, 67.
Chiu, Y. T., Luhmann, J. G., Ching, B. K., and Boucher, D. J. 1979, *J. Geophys. Res.*, **84**, 909.
Cohn, H., and York, D. G. 1977, *Ap. J.*, **216**, 408.
Cowie, L. L., Taylor, W., and York, D. G. 1981, *Ap. J.*, **248**, 528.
Cruddace, R., Paresce, F., Bowyer, S., and Lampton, M. 1974, *Ap. J.*, **187**, 497.
Crutcher, R. M. 1982, *Ap. J.*, **254**, 82.
Flamand, J., Passereau, G. and Thevenon, A. 1977, *Proc. 5th Conf. on Vacuum UV Rad. Physics, Montpellier*, Vol. **III**, p. 45.
Frisch, P. D. 1981, *Nature*, in press.
Greenstein, J. L., and Oke, J. B. 1979, *Ap. J.* (*Letters*), **229**, L141.
Griem, H. R. 1974, *Spectral Line Broadening by Plasmas* (New York: Academic Press).
Heiles, C. 1975, *Astr. Ap. Suppl.*, **20**, 37.
Heise, J., and Huizenga, H. 1980, *Astr. Ap.*, **84**, 280.
Holberg, J. B., Sandel, B. R., Forrester, W. T., Broadfoot, A. L., Shipman, H. L., and Barry, J. L. 1980, *Ap. J.* (*Letters*), **242**, L119.
Jacchia, L. G. 1971, *Smithsonian Ap. Obs. Spec. Rept., No. 332, Revised Static Models of the Thermosphere and Exosphere with Empirical Temperature Profiles.*
Knude, J. 1979, *Astr. Ap.*, **77**, 198.
Lampton, M., Cash, W., Malina, R. F. and Bowyer, S. 1977, *Proc. Sci. Photo-Opt. Instr. Eng.*, **106**, 93.
Lampton, M., Margon, B. and Bowyer, S. 1976, *Ap. J.*, **208**, 177.
Lampton, M., Margon, B., Paresce, F., Stern, R. and Bowyer, S. 1976, *Ap. J.* (*Letters*), **203**, L71.
Lampton, M. and Paresce, F. 1974, *Rev. Sci. Instr.*, **45**, 1098.

Lang, K. R. 1974, *Astrophysical Formulae* (Berlin: Springer-Verlag).
Liebert, J., Gresham, M., Hege, E. K., and Strittmatter, P. A. 1979, *A.J.*, **84**, 1612.
Mack, J., Paresce, F., and Bowyer, S. 1976, *Appl. Optics*, **15**, 861.
Malina, R. F. 1979, Ph.D. thesis, University of California, Berkeley.
Malina, R. F., Basri, R., and Bowyer, S. 1982, *Bull. AAS*, **13**, 873.
Malina, R. F., Bowyer, S., Finley, D. and Cash, W. 1980, *Opt. Engineering*, **19**, 211.
Margon, B., Liebert, J., Gatewood, G., Lampton, M., Spinrad, H., and Bowyer, S. 1976, *Ap. J.*, **209**, 525.
McKee, C. F., and Cowie, L. L. 1977, *Ap. J.*, **215**, 213.
Mihalas, D. 1978, *Stellar Atmospheres* (San Francisco: W. H. Freeman).
Muchmore, D. 1982, *Ap. J.*, **259**, 749.
Muchmore, D. O., and Böhm, K. H. 1978, *Astr. Ap.*, **69**, 113.
Paresce, F., and Stern, R. 1981, *Ap. J.*, **247**, 89.
Paresce, F., Fahr, H., and Lay, G. 1981, *J. Geophys. Res.*, in press.
Schatzman, E. 1958, *White Dwarfs* (Amsterdam: North-Holland).
Shapiro, P. R., and Moore, R. T. 1976, *Ap. J.*, **207**, 460.
Shipman, H. L. 1972, *Ap. J.*, **177**, 723.
_____. 1979, *Ap. J.*, **228**, 240.
Shull, J. M., and McKee, C. F. 1979, *Ap. J.*, **227**, 131.
Tinbergen, J. 1982, *Astr. Ap.*, **105**, 53.
Weaver, H. 1979, in *IAU Symposium 84, The Large Scale Characteristics of the Galaxy*, ed. W. B. Burton (Dordrecht: Reidel), p. 295.
Weller, C. S., and Meier, R. R. 1981, *Ap. J.*, **246**, 386.
Wesemael, F. 1981, *Ap. J.*, **247**, 590.
Wesemael, F., Auer, L. H., Van Horn, H. M., and Savedoff, M. P. 1980, *Ap. J. Suppl.*, **43**, 159.
Wesselius, P. R., and Koester, D. 1978, *Astr. Ap.*, **70**, 745.
York, D. B., and Kinahan, B. F. 1979, *Ap. J.*, **228**, 127.

GIBOR BASRI, STUART BOWYER, and ROGER F. MALINA: Space Sciences Laboratory, University of California, Berkeley, Berkeley, CA 94720